Physical and functional association of migfilin with cell-cell adhesions

Vasiliki Gkretsi[1,*], Yongjun Zhang[1,*], Yizeng Tu[1], Ka Chen[1], Donna B. Stolz[2], Yanqiang Yang[1], Simon C. Watkins[2] and Chuanyue Wu[1,‡]

[1]Department of Pathology and [2]Department of Cell Biology and Physiology, Center for Biological Imaging, University of Pittsburgh, Pittsburgh, PA 15261, USA

*These authors contributed equally to this work
‡Author for correspondence (e-mail: carywu@pitt.edu)

Accepted 8 November 2004
Journal of Cell Science 118, 697-710 Published by The Company of Biologists 2005
doi:10.1242/jcs.01638

Summary

Cell-cell junctions are essential for epithelial and endothelial tissue formation and communication between neighboring cells. We report here that migfilin, a recently identified component of cell-extracellular matrix adhesions, is recruited to cell-cell junctions in response to cadherin-mediated cell-cell adhesions. Migfilin is detected at cell-cell junctions in both epithelial and endothelial cells. It forms detergent-resistant, discrete clusters that associate with actin bundles bridging neighboring cells. Immunoelectron microscopic analyses reveal that migfilin is closely associated with β-catenin, but not desmosomes, at cell-cell junctions. Furthermore, we show that the C-terminal LIM domains, but not its N-terminal domain, mediates migfilin localization to cell-cell junctions. The site mediating the localization of migfilin to cell-cell junctions at least partially overlaps with that mediating the localization of migfilin to cell-ECM adhesions. Finally, siRNA-mediated depletion of migfilin compromised the organization of adherens junctions and weakened cell-cell association. These results identify migfilin as a component of adherens junctions and suggest an important role for migfilin in the organization of the cell-cell adhesion structure.

Key words: Migfilin, Catenin, Mig-2, Cell-cell junctions, Cell-extracellular matrix adhesions, Actin cytoskeleton

Introduction

Cell-cell and cell-extracellular matrix (ECM) adhesions are constituently and functionally distinct subcellular structures that are essential for the assembly of cells into tissues, and for communication between neighboring cells and between cells and the ECM. Cell-cell and cell-ECM adhesions are mediated primarily by transmembrane adhesion receptors of different families (i.e. cadherin and integrin) and multiple cytoplasmic protein-protein interactions, which, among other things, connect the plasma membrane to the actin cytoskeleton (Burridge and Chrzanowska-Wodnicka, 1996; Yap et al., 1997; Adams and Nelson, 1998; Liu et al., 2000; Geiger et al., 2001; Hynes, 2002; Jamora and Fuchs, 2002). The membrane-actin cytoskeleton connections enable cells to respond in a coordinated manner to signals from neighboring cells and the ECM and to efficiently modulate their behavior, including shape, motility and gene expression – properties essential for fundamental physiological processes such as morphogenesis, differentiation and growth. Identification of the molecular constituents of cell-cell and cell-ECM adhesions and the structural determinants that control their localization to these two distinct subcellular adhesion structures are therefore of fundamental importance.

Migfilin is a recently identified and cloned protein that is a component of cell-ECM adhesions, where it links the cell-ECM adhesions to the actin cytoskeleton and functions in actin cytoskeleton remodeling and cell shape modulation (Tu et al., 2003). Migfilin is recruited to cell-ECM adhesions by Mitogen-inducible gene-2 (*MIG-2*) (Tu et al., 2003), a human homologue of the *Caenorhabditis elegans* focal adhesion protein UNC-112, which is indispensable for cell-ECM adhesion assembly (Rogalski et al., 2000). In addition, migfilin interacts with filamin (Takafuta et al., 2003; Tu et al., 2003) and vasodilator-stimulated phosphoprotein (VASP) (Y.Z., Y.T. and C.W., unpublished observation), actin-binding proteins that are crucial for actin cytoskeleton organization and processes that require extensive shape modulation (e.g. migration) (reviewed by Krause et al., 2003; Stossel et al., 2001; van der Flier and Sonnenberg, 2001). Migfilin consists of five domains: a filamin-binding N-terminal domain, a VASP-binding proline-rich domain that also contains a nuclear export signal, and three LIM domains at the C-terminal region that mediate the interaction with Mig-2. The LIM domain is a protein-binding motif consisting of a cysteine-rich consensus sequence of approximately 50 amino acids that fold into a specific threedimensional structure comprising two zinc-fingers (Dawid et al., 1998; Jurata and Gill, 1998; Schmeichel and Beckerle, 1994). A splice variant of migfilin, migfilin(s), is co-expressed with migfilin in several cell types and tissues (Tu et al., 2003). Migfilin(s) is identical to migfilin except that it lacks the central proline-rich domain.

In the present study, we show that migfilin not only localizes to cell-ECM adhesions but also is recruited to cell-cell junctions in epithelial and endothelial cells. Using

a combination of biochemical, cell biological, immunofluorescence and immunoelectron microscopic approaches, we have characterized the ultrastructure of the migfilin-containing structures at cell-cell junctions. In addition, we have identified the determinants that control migfilin localization to cell-cell and cell-ECM adhesions. Finally, we have investigated the function of migfilin in cell-cell junctions by RNA interference. Our results identify a new component of adherens junctions and suggest an important role of migfilin in the organization of the cell-cell adhesion structure.

Materials and Methods

Cell lines and antibodies

Primary newborn human embryonic keratinocytes (NHEK) (Clonetics) were cultured in KBM-2 medium containing the supplements recommended by the company. Primary human microvascular endothelial cells (HMVEC) were purchased from Clonetics and cultured in EGM-MV medium (Clonetics). HaCat and MCF-7 cells were cultured in DMEM medium containing 10% fetal bovine serum (FBS), 1% Glutamax, and 1% penicillin/streptomycin. Human HT-1080 fibrosarcoma cells were cultured in modified Eagle's medium (MEM) supplemented with L-glutamine, 10% FBS, and non-essential amino acids. Mouse monoclonal antibodies recognizing migfilin and Mig-2 were generated as described previously (Tu et al., 2003). Rabbit polyclonal anti-β-catenin antibody and mouse monoclonal anti-pan-cadherin antibody (clone CH-19) were purchased from Sigma. Rabbit polyclonal anti-FAK antibody was purchased from Santa Cruz. Mouse monoclonal anti-E-cadherin antibody (SHE78-7) was from Calbiochem. Rhodamine Red™- or FITC-conjugated anti-mouse IgG antibodies and Rhodamine Red™-conjugated anti-rabbit IgG antibodies were purchased from Jackson ImmunoResearch Laboratories. In some immunofluorescent staining experiments (Fig. 3), a goat anti-mouse Alexa 488 antibody (Molecular Probes, Eugene, OR) and a goat anti-rabbit Cy3 (Jackson Immunolabs) were used as secondary antibodies.

Migfilin expression vectors, site-directed mutagenesis and DNA transfection

The expression vectors encoding green fluorescent protein (GFP)-tagged migfilin, the short form splicing variant of migfilin that lacks the proline-rich domain [migfilin(s)], and deletion mutants of migfilin (as specified in each experiment) were generated by inserting the corresponding cDNA fragments into pEGFP-C2 vector (Clontech). Point mutations were generated by PCR using the Pfu DNA polymerase from Invitrogen, and the QuickChange™ site-directed mutagenesis system from Stratagene. All mutations were confirmed by DNA sequencing. HaCat cells were transfected with expression vectors encoding GFP-tagged wild-type and mutant forms of migfilin with LipofectAmine PLUS (Life Technologies), following the manufacturer's protocol.

Immunofluorescent staining and confocal microscopy

Immunofluorescent staining was performed as described previously (Tu et al., 2003; Zhang et al., 2002). Briefly, cells were plated on fibronectin-coated coverslips, fixed with 4% paraformaldehyde and incubated at room temperature with appropriate primary and secondary antibodies or Rhodamine-conjugated phalloidin as specified in each experiment. In experiments in which cells were transfected with GFP-migfilin expression vectors, Rhodamine Red™-conjugated secondary anti-mouse or anti-rabbit IgG antibodies were used. In double-staining experiments with mouse anti-migfilin antibody and rabbit anti-β-catenin antibody or mouse anti-pan-cadherin antibody and rabbit anti-β-catenin antibody, FITC-conjugated anti-mouse IgG and Rhodamine Red™-conjugated anti-rabbit IgG secondary antibodies were used. The cells were observed either under a Leica DM R fluorescence microscope or an Olympus Fluoview BX61 confocal microscope.

Cytoskeletal extraction

Cytoskeletal extractions of cells were performed essentially as described previously (Heuser and Kirschner, 1980). Briefly, with all solutions at 37°C, cells on 12 mm round glass coverslips were washed with cytoskeletal buffer (100 mM PIPES, pH 6.9, 0.1 mM EDTA, 0.5 mM $MgCl_2$, 4 M glycerol, 1:100 dilution mammalian protease inhibitor cocktail) (Sigma), and then extracted with cytoskeletal buffer supplemented with 0.75% Triton X-100 for 3 minutes with one change of the extraction buffer during this time period. Extracted cells were washed once with cytoskeletal buffer, and then fixed in cytokeletal buffer supplemented with 2% paraformaldehyde for 1 hour. Cells were stored in PBS at 4°C until use.

Cationic colloidal silica unroofing of cells

Cells were unroofed as described previously (Stolz and Jacobson, 1992). All isolation solutions were maintained at 4°C. Briefly, cells were washed in MES-buffered saline (MBS: 20 mM morpholinoethane sulfonic acid, 135 mM NaCl, 0.5 mM $CaCl_2$, 1 mM $MgCl_2$) and were then overcoated with a 1% solution of cationic colliodal silica, which was prepared as a 30% stock colloid as described previously (Chaney and Jacobson, 1983). Cells were subsequently washed with MBS, overcoated with 1% polyacrylic acid in MBS (stock 25% aqueous polyacrylic acid solution, ave. mol. wt. 100,000) (Aldrich, St Louis, MO). Then, cells were washed with MBS and they were allowed to swell in hypotonic lysis buffer for 10 minutes (lysis buffer: 2.5 mM imidizole, pH 7.0, supplemented with protease inhibitors (1:100 dilution mammalian protease inhibitor cocktail) (Sigma). Cells were then unroofed by squirting the monolayers with lysis buffer through a 5 ml syringe fitted with a blunted, flattened 18 gauge needle. The degree of lysis was monitored by observing cells on an inverted microscope. Footprints were washed once with MBS and fixed in 2% paraformaldehyde in PBS for 1 hour and stored in PBS at 4°C until use. (Cationic colloidal silica can be obtained by written request from Donna Beer Stolz, University of Pittsburgh, Pittsburgh, PA 15261, e-mail: dstolz@pitt.edu.)

Immunoelectron microscopy

HaCat cells were fixed in cryofix (2% paraformaldehyde, 0.01% glutaraldehyde in 0.1 M PBS) and stored at 4°C for 1 hour. Cells were pelleted and resuspended in a small amount of 3% gelatin in PBS, solidified at 4°C then fixed for an additional 15 minutes in cryofix. Gelatin-cell block was cryoprotected in PVP cryoprotectant overnight at 4°C [25% poly(vinylpyrrolidone), 2.3 M sucrose, 0.055 M Na_2CO_3, pH 7.4 (Tokuyasu, 1989)]. Cell blocks were frozen on ultracryotome stubs under liquid nitrogen and stored in liquid nitrogen until use. Ultrathin sections (70-100 nm) were cut using a Reichert Ultracut U ultramicrotome with a FC4S cryo-attachment, lifted on a small drop of 2.3 M sucrose and mounted on Formvar-coated copper grids. Sections were washed three times with PBS, then three times with PBS containing 0.5% bovine serum albumin and 0.15% glycine (PBG buffer); this was followed by a 30 minute blocking incubation with 5% normal goat serum in PBG. Sections were labeled with a rabbit anti-β-catenin antiserum (1:100) and the ascites fluid of the mouse monoclonal anti-migfilin antibody (clone 43) (1:100) in PBG for 1 hour. Sections were washed four times in PBG and labeled with goat anti-rabbit (10 nm) or goat anti-mouse (5 nm) gold conjugated secondary antibodies (Amersham), each at a dilution of 1:25 for 1 hour. Sections were washed three times in PBG, three times in PBS then fixed in 2.5% glutaraldehyde in PBS for 5 minutes, washed twice

in PBS then washed six times in ddH_2O. Sections were post-stained in 2% neutral uranyl acetate for 7 minutes, washed three times in ddH_2O, stained for 2 minutes in 4% uranyl acetate then embedded in 1.25% methyl cellulose. Labeling was observed on a JEOL JEM 1210 electron microscope (Peabody, MA) at 80 kV.

Pre-embedding immuno-transmission microscopy

HaCat cells were grown on 35 mm tissue culture plates, the cytoskeleton was extracted as described above and cells were fixed with 2% paraformaldehyde in PBS for 1 hour. Cells were then washed three times with PBS and three times with PBG. Following this washing step, cells were blocked in 20% normal goat serum in PBG for 40 minutes and were then washed once with PBG. Primary antibodies were added to cells in PBG and incubated at room temperature for 4 hours. Cells were washed four times in PBG and secondary antibodies conjugated to gold (goat anti-rabbit, 5 nm; goat anti-mouse, 10 nm) (Amersham) were added to the cells overnight at 4°C. Cells were then washed three times in PBG and three times in PBS, and they were fixed in 2.5% glutaraldehyde for 1 hour. Another wash step in PBS followed and cells were then post-fixed in 1% aqueous osmium tetroxide for 1 hour. They were subsequently washed in PBS and were dehydrated through a 30-100% ethanol series and several changes of Polybed 812 embedding resin (Polysciences, Warrington, PA). Cultures were embedded in by inverting Polybed 812-filled BEEM capsules on top of the cells. Blocks were cured overnight at 37°C, and then cured for two additional days at 65°C. Monolayers were pulled off the tissue culture plates. Ultrathin en face sections (60 nm) of the cells were obtained on a Riechart Ultracut E microtome, post-stained in 4% uranyl acetate for 10 minutes and 1% lead citrate for 7 minutes. Sections were finally viewed on a JEOL JEM 1210 transmission electron microscope (JEOL, Peobody MA) at 80 kV.

Calcium chelation assays

The calcium chelation assay was essentially performed as described previously (Helwani et al., 2004; Rothen-Rutishauser et al., 2002). Briefly, MCF-7 cells were plated on fibronectin-coated coverslips; they were allowed to attach and were then subject to serum starvation for 18 hours. The medium was then switched to DMEM supplemented with 4 mM EGTA and 1 mM $MgCl_2$, and the cells were incubated at 37°C for 30 minutes. Cells were then washed twice with PBS and the medium was changed back to the regular calcium-containing culture medium. After incubation for periods of time as specified, cells were fixed and dually stained with mouse anti-migfilin antibody and rabbit anti-β-catenin antibody.

In some experiments, MCF7 mammary epithelial cells were transiently transfected with an expression vector encoding GFP-migfilin using LipofectaminePLUS. Twenty four hours following the transfection, cells were plated on fibronectin-coated coverslips and were then subject to serum starvation for 18 hours. The medium was then changed to DMEM supplemented with 4 mM EGTA, 1 mM $MgCl_2$ and a function-blocking mouse monoclonal anti E-cadherin antibody (SHE78-7, 4 μg/ml) or an irrelevant mouse IgG (4 μg/ml) as a control. The cells were incubated at 37°C for 1 hour and washed twice with PBS; the medium was then switched back to the normal culture medium, which again contained 4 μg/ml of either the function-blocking anti-E-cadherin antibody or the irrelevant control mouse IgG antibody. One hour following the switch to the normal calcium-containing medium, cells were fixed with 4% paraformaldehyde and stained with a rabbit polyclonal anti-β-catenin antibody and a Rhodamine Red™-conjugated anti-rabbit IgG antibody.

RNA interference

Human HT-1080 fibrosarcoma cells were transfected with an siRNA that specifically targets migfilin mRNA (sense sequence: 5′-AAAGGGGCAUCCACAGACAUC-3′), or a 21-nucleotide irrelevant RNA as a control, as previously described (Tu et al., 2003). The cells were analyzed by western blotting, immunofluorescent staining or cell dissociation assays 2 days after siRNA transfection.

Cell dissociation assay

Cell dissociation assay was performed following a previously published method (Takeda et al., 1995). Briefly, the cells (as specified in each experiment) were detached from culture plates with a rubber policeman and passed through glass Pasteur pipettes ten times. The cells were then fixed in 1% glutaraldehyde and pictures were taken under an Olympus IX70 inverted microscope equipped with a MagnaFire™ digital camera. The extent of cell dissociation was represented by the ratio of the number of particles (Np) over the number of cells (Nc) (Np/Nt). The values of Np/Nc were calculated by analyzing at least 500 cells from each sample.

Results

Migfilin is a component of cell-cell junctions in epithelial and endothelial cells

Epithelial cells are attached not only to ECM but also to neighboring cells via highly specialized subcellular structures termed cell-cell junctions. To analyze the subcellular localization of migfilin in epithelial cells, we immunofluorescently stained human primary keratinocytes with a monoclonal antibody that specifically recognizes migfilin (Tu et al., 2003). Clusters of migfilin (Fig. 1A, arrows) were detected at cell-cell junctions where abundant β-catenin (Fig. 1B) and E-cadherin (not shown), which are well-described components of cell-cell junctions, were present. As expected, migfilin clusters were also detected at cell-ECM adhesions (Fig. 1A, arrowheads) lacking β-catenin (Fig. 1B) and E-cadherin (not shown). Colocalization of migfilin with β-catenin and E-cadherin at cell-cell adhesions was also observed in immortalized HaCat keratinocytes (not shown). Double staining of the human keratinocytes with the mouse monoclonal anti-migfilin antibody and a rabbit polyclonal anti-FAK antibody confirmed that migfilin was clustered at both cell-ECM adhesions (Fig. 1C, arrowheads) where FAK was concentrated (Fig. 1D) and cell-cell adhesions (Fig. 1C, arrows) that lacked FAK (Fig. 1D). The localization of migfilin to both cell-cell and cell-ECM adhesions has also been observed in other epithelial cells that have been analyzed, including human mammary epithelial cells and Madin-Darby canine kidney epithelial cell (not shown).

To test whether migfilin localizes to cell-cell junctions in endothelial cells, another major type of cells that assemble both cell-cell and cell-ECM junctions, we stained primary human microvascular endothelial cells with the monoclonal anti-migfilin antibody. As in epithelial cells, migfilin was clustered at both cell-cell junctions (Fig. 1E, arrows), where abundant β-catenin was detected (Fig. 1F), and cell-ECM adhesions (Fig. 1E, arrowheads) that lacked β-catenin (Fig. 1F).

To confirm that migfilin colocalizes with β-catenin at cell-cell adhesions, we analyzed human keratinocytes by confocal immunofluorescence microscopy. The results showed that migfilin was co-clustered with β-catenin at lateral cell-cell junctions (Fig. 2A-C,G). Clusters of migfilin were also detected at basal cell-ECM adhesions where β-catenin was not concentrated (Fig. 2D-G).

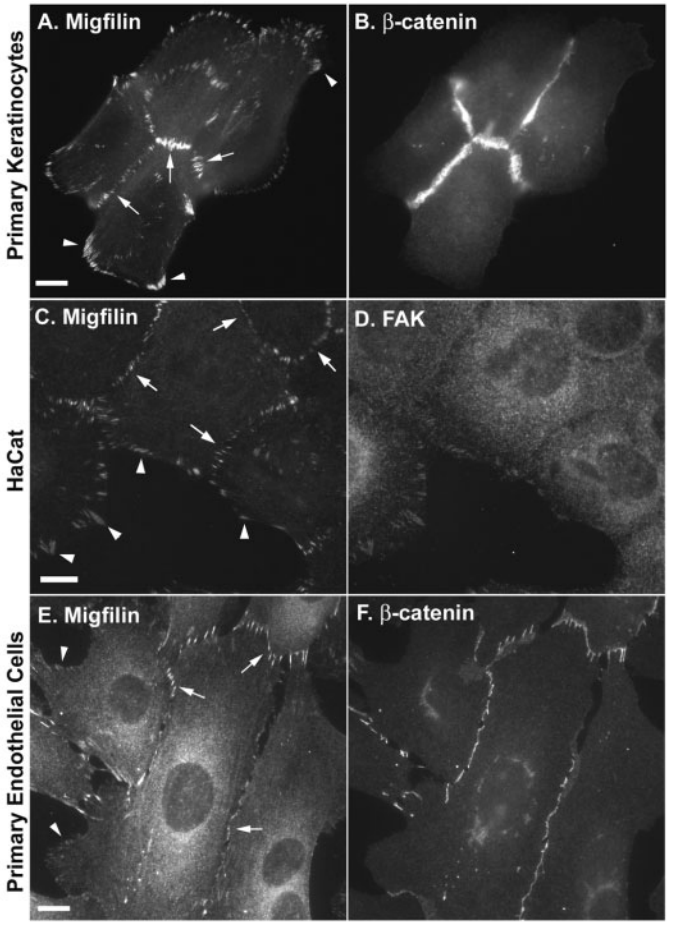

Fig. 1. Migfilin localizes to cell-cell junctions in epithelial and endothelial cells. (A-D) Primary newborn human embryonic keratinocytes (A and B), immortalized human keratinocytes (HaCat) (C and D) and primary human microvascular endothelial cells (E and F) were double stained with a mouse monoclonal anti-migfilin antibody (clone 43) (A, C and E) and a rabbit polyclonal anti-β-catenin antibody (B and F) or anti-FAK antibody (D). The images were recorded using a Leica DM R fluorescence microscope equipped with a Hamamatsu ORCA-ER digital camera. The cell-cell and cell-ECM adhesions are indicated by arrows and arrowheads, respectively. Note that a fraction of migfilin was co-clustered with β-catenin at cell-cell junctions (arrows, C) that lack FAK (D). Migfilin was also detected at FAK-rich cell-ECM adhesions (arrowheads, C and D). Bars in A, C and E, 8 μm.

Migfilin forms detergent-resistant clusters that associate with actin bundles at cell-cell junctions

We next sought to characterize the association of migfilin with cell-cell junctions. We first tested whether migfilin could be removed from cell-cell junctions by extraction with nonionic detergents. To do this, we extracted HaCat cells with a Triton X-100-containing buffer. Analyses of the Triton X-100-extracted cells showed that migfilin remained to associate with β-catenin at cell-cell adhesions (Fig. 3A-C, arrowheads). Furthermore, double staining of the cells with anti-migfilin monoclonal antibody and phalloidin showed that migfilin was co-clustered with the anchoring sites of filamentous actin at cell-cell junctions, forming discrete structures that appeared to bridge neighboring cells (Fig. 3D).

It is well known that in epithelial cells, filamentous actin forms a network (Fig. 3G) linking the basal ECM adhesions with lateral cell-cell junctions, and the latter supports the connections between neighboring cells and the formation of epithelial sheets. To confirm that the migfilin clusters are physically associated with these two (basal cell-ECM adhesions and lateral cell-cell adhesions) adhesion structures, we physically separated cell-cell and cell-ECM adhesions using a cationic colloidal silica 'unroofing' protocol (Stolz and Jacobson, 1992). Staining of the 'unroofed' cells showed that migfilin clusters at cell-cell-junctions were removed with the apical and lateral plasma membrane and the actin bundles that were anchored, whereas migfilin clusters at the basal ECM adhesions (or 'cell footprints') and the associated filamentous actin remained (Fig. 3E,I). Additionally, the association of migfilin with the basal ECM adhesions, like that of migfilin with cell-cell junctions, resisted nonionic detergent extraction (Fig. 3F).

Immunoelectron microscopic analyses of migfilin clusters at cell-cell junctions

To define the localization and ultrastructure of migfilin at cell-cell junctions at higher magnification, we analyzed the cells by immunoelectron microscopy. Consistent with the immunofluorescent confocal microscopic results (Fig. 2), immunoelectron microscopic analysis of unextracted HaCat cells showed that migfilin is localized in the vicinity of β-catenin at cell-cell contacts (Fig. 4A). To visualize filamentous actin and further test whether migfilin is closely associated with filamentous actin and β-catenin, we extracted the cells with a Triton X-100-containing buffer and analyzed them by pre-embedding immunotransmission microscopy as described in Materials and Methods. The results showed that, consistent with the immunofluorescent microscopic analyses (Fig. 3), migfilin associated with actin bundles that linked neighboring cells (Fig. 4B, arrows). The migfilin clusters (Fig. 4C, arrowheads) were not associated with desmosomes (Fig. 4C, arrows). Furthermore, double staining of cells with anti-migfilin and anti-β-catenin antibodies showed that migfilin was closely associated with β-catenin (often within 100 nm), and they formed electron dense, compact complexes that appeared to clamp actin bundles (Fig. 4D). These results suggest that migfilin forms a complex with both β-catenin and filamentous actin at adherens junctions.

The recruitment of migfilin to cell-cell junctions is temporally separable from that of β-catenin

To analyze the temporal relation between migfilin and β-catenin recruitment to adherens junctions, we disassembled the adherens junctions by treating epithelial cells with a calcium-chelator (EGTA), and then added back medium that contains calcium, which is known to induce E-cadherin-mediated adherens junction assembly (Nagafuchi et al., 1987). The epithelial cells were fixed at different time points after switching to calcium-containing medium. Immunofluorescence staining analysis with anti-migfilin and anti-β-catenin antibodies showed that β-catenin was clustered at adherens junctions within 15 minutes from the calcium-switch (Fig. 5A), whereas at the same time point migfilin was

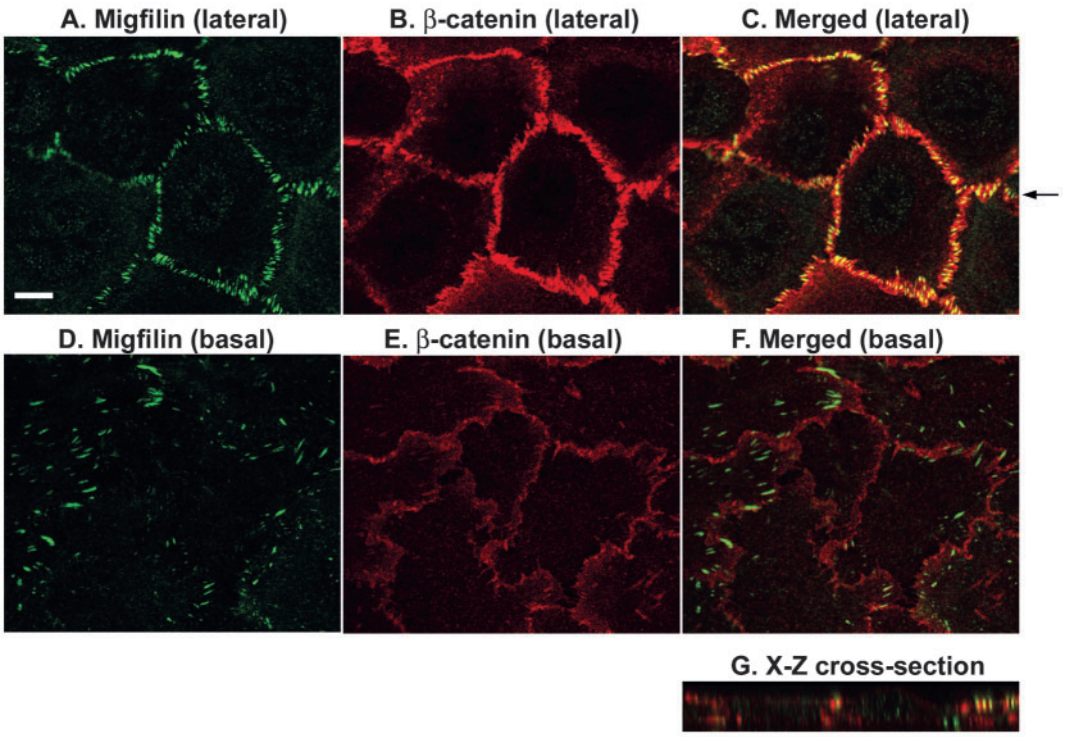

Fig. 2. Immunofluorescent confocal microscopic analysis of cell-cell adhesion localization of migfilin. Human immortalized keratinocytes (HaCat cells) were double stained with monoclonal anti-migfilin antibody (clone 43) (A and D) and a rabbit polyclonal anti-β-catenin antibody (B and E) observed under an Olympus Fluoview BX61 confocal microscope. The *x*-*z* sections at the lateral (A and B) and basal (D and E) levels were shown. (C,F) Images merged from the migfilin (green) and β-catenin (red) staining at the lateral and basal levels, respectively. The arrow in C indicates the position of the *x*-*z* cross section (G). Bar, 8 μm.

not clustered at adherens junctions (Fig. 5B). Soon after the clustering of β-catenin (30 minutes from the calcium-switch), however, migfilin (Fig. 5D) was recruited to the adherens junctions where β-catenin (Fig. 5C) clusters were detected. Thus, the recruitment of migfilin to the adherens junctions appears to be temporally separable from that of β-catenin, which has been shown to be co-recruited with E-cadherin from ER to adherens junctions (Chen et al., 1999).

The recruitment of migfilin to cell-cell junctions depends on cadherin-mediated cell-cell adhesion

To test whether the localization of migfilin to cell-cell junctions depends on cadherin, we treated MCF-7 cells with a function-blocking mouse monoclonal anti-E-cadherin antibody (SHE78-7). Because the presence of the mouse monoclonal anti-E-cadherin antibody obscures the immunofluorescent detection of migfilin using the mouse anti-migfilin antibody, we transfected MCF-7 cells with an expression vector encoding GFP-migfilin and analyzed the effect of the function-blocking anti-E-cadherin antibody on the localization of GFP-migfilin. Consistent with the results obtained with the monoclonal anti-migfilin antibody (Fig. 5C,D), GFP-migfilin was readily recruited to β-catenin-rich cell-cell adhesions in MCF-7 cells that were incubated with the control mouse IgG (Fig. 5E,F). By marked contrast, in MCF-7 cells that were incubated with the function-blocking anti-E-cadherin antibody, no GFP-migfilin clusters were detected at the cell-cell boundaries (Fig. 5G,H). The presence of the function-blocking anti-E-cadherin antibody, however, did not prevent the recruitment of GFP-migfilin to cell-ECM adhesions (Fig. 5I,J). Thus, the recruitment of migfilin to cell-cell junctions, but not that of migfilin to cell-ECM adhesions, depends on cadherin-mediated cell-cell adhesion.

Cell-cell adhesion, cell-ECM adhesion and nuclear localization of migfilin(s)

We next tested whether migfilin(s), a naturally occurring splicing variant of migfilin that lacks the central proline-rich domain (Tu et al., 2003), localizes to adherens junctions. To do this, we transfected HaCat cells with expression vectors encoding GFP-migfilin(s), and GFP-migfilin as a control. The expression of GFP-migfilin and GFP-migfilin(s) in the corresponding transfectants was confirmed by western blotting (Fig. 6A, lanes 1 and 2). Immunofluorescence analysis showed that GFP-migfilin(s) (Fig. 7C), like GFP-migfilin (Fig. 7A), colocalized with β-catenin at cell-cell junctions (Fig. 7B,D). A fraction of GFP-migfilin(s) was also detected in the nuclei (Fig. 7C, also see Fig. 9C), whereas GFP-migfilin was largely absent in the nuclei (Fig. 7A), which is consistent with the presence of a nuclear export signal in the central proline-rich domain (Akazawa et al., 2004; Takafuta et al., 2003). These results suggest that the central proline-rich domain is not required for the localization of migfilin to adherens junctions, albeit it plays an important role in the regulation of the nuclear localization of migfilin.

The C-terminal LIM domains, but not the N-terminal filamin-binding domain, mediate migfilin localization to cell-cell junctions

In addition to the central proline-rich domain, migfilin contains an N-terminal filamin-binding domain and a Mig-2-binding C-terminal region that consists of three LIM domains. To determine which of the migfilin regions mediates migfilin localization to adherens junctions, we generated expression vectors encoding GFP-tagged migfilin N-terminal domain (GFP-N-Ter), the proline-rich and the C-terminal LIM domains (GFP-PR-LIM1-3) and the C-terminal LIM domains (GFP-

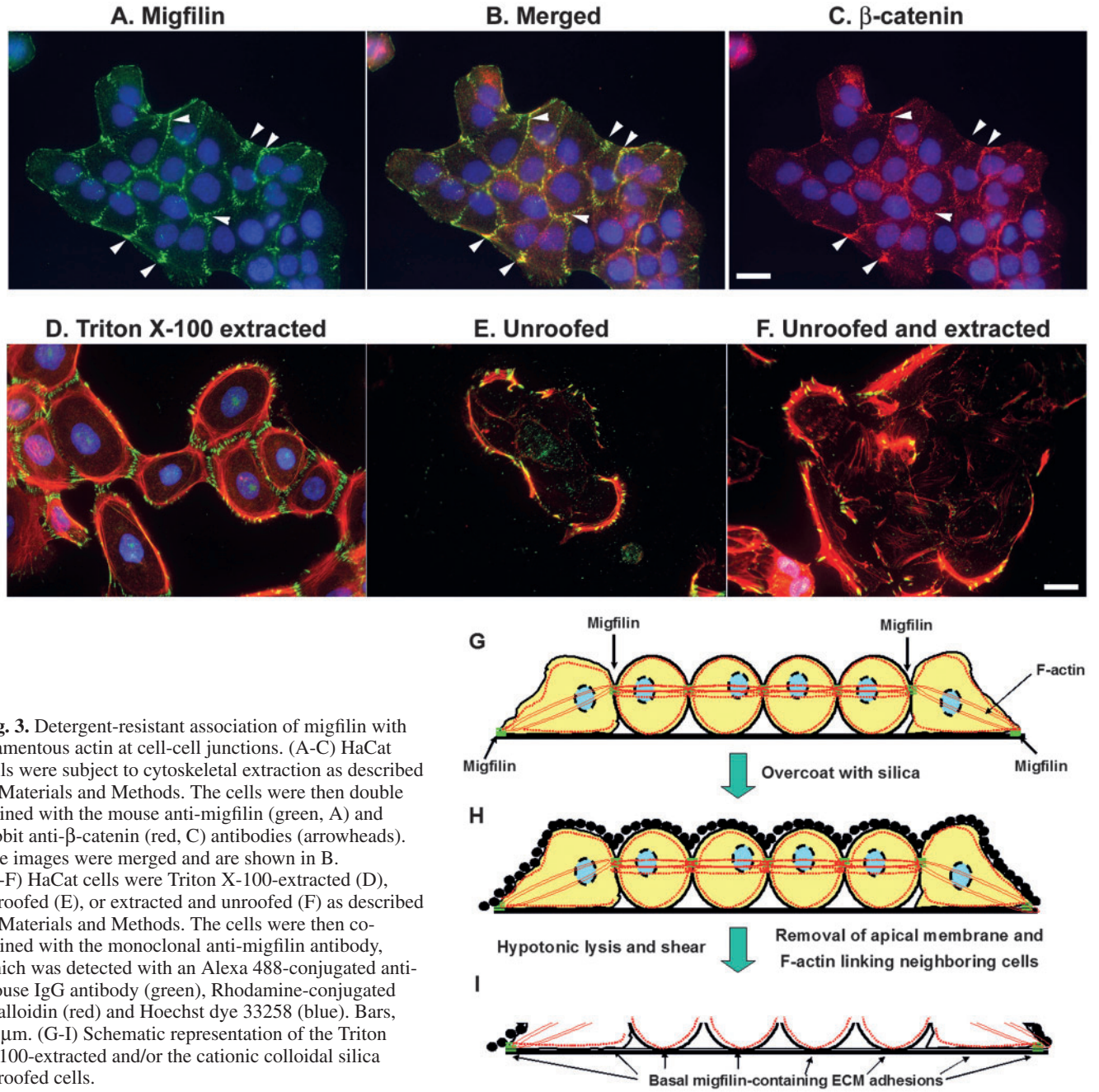

Fig. 3. Detergent-resistant association of migfilin with filamentous actin at cell-cell junctions. (A-C) HaCat cells were subject to cytoskeletal extraction as described in Materials and Methods. The cells were then double stained with the mouse anti-migfilin (green, A) and rabbit anti-β-catenin (red, C) antibodies (arrowheads). The images were merged and are shown in B. (D-F) HaCat cells were Triton X-100-extracted (D), unroofed (E), or extracted and unroofed (F) as described in Materials and Methods. The cells were then co-stained with the monoclonal anti-migfilin antibody, which was detected with an Alexa 488-conjugated anti-mouse IgG antibody (green), Rhodamine-conjugated phalloidin (red) and Hoechst dye 33258 (blue). Bars, 25 μm. (G-I) Schematic representation of the Triton X-100-extracted and/or the cationic colloidal silica unroofed cells.

LIM1-3) (Fig. 6B). HaCat cells were transfected with the GFP expression vectors encoding the different domains of migfilin. The expression of the GFP-tagged migfilin fragments in the corresponding transfectants was confirmed by western blotting (Fig. 6A, lanes 3-5). Analysis of the subcellular localization of the GFP-tagged migfilin mutants showed that GFP-PR-LIM1-3 (Fig. 7E), like GFP-migfilin (Fig. 7A), was clustered at cell-cell junctions where abundant β-catenin was present (Fig. 7F), indicating that the N-terminal domain is not required for migfilin localization to cell-cell junctions. Clusters of GFP-LIM1-3 were also detected at β-catenin-rich adherens junctions (Fig. 7G,H), suggesting that the C-terminal LIM domains are sufficient for mediating migfilin localization to adherens junctions. By contrast, the N-terminal fragment was not clustered at cell-cell junctions but instead it associated primarily with the actin filaments (Fig. 7I,J). Taken together, these results suggest that the C-terminal LIM domains, but not the N-terminal domain, mediate migfilin localization to cell-cell junctions.

The LIM 2 domain is essential for migfilin clustering at cell-cell adhesions

To identify the LIM domain within the C-terminal region that is essential for mediating migfilin localization to cell-cell junctions, we introduced mutations into different migfilin LIM domains (Fig. 6B) and expressed the GFP-tagged migfilin mutants in HaCat cells (Fig. 6A, lanes 6-10). GFP-ΔLIM1N,

in which the first zinc finger in the LIM1 domain was deleted (Fig. 6B), was able to cluster at cell-cell junctions (Fig. 8A,B), suggesting that the first zinc finger of LIM1 domain is not absolutely required for migfilin clustering at these sites. Noticeably, GFP-ΔLIM1N also accumulated in the nuclei (Fig. 8A). However, substitution of C243 or C291 - which are crucial for the folding of the LIM2 domain (Fig. 6B) - with Gly eliminated the clustering of migfilin at cell-cell junctions, although they were still capable of associating with the actin filaments (Fig. 8C-F). Thus, the LIM2 domain is essential for migfilin clustering at cell-cell junctions. We next analyzed the localization of migfilin or migfilin(s) mutants bearing a point mutation at C306, which is essential for the folding of the first zinc finger of LIM3 (Fig. 6B). The localization of migfilin(s) C306→G point mutant (Fig. 8G,H, arrows) or that of migfilin C306→G point mutant (not shown) to the β-catenin-containing cell-cell adhesions was compromised, suggesting that LIM3 also plays an important role in the recruitment of migfilin to these sites. The C306→G point mutants (Fig. 8G), like the C243→G (Fig. 8C) and the C291→G (Fig. 8E) mutants, efficiently associated with the actin filaments, which is reminiscent of that of migfilin N-terminal fragment (Fig. 7I). The migfilin(s) C306→G point mutant (Fig. 8G), but not migfilin C306→G point mutant that contains the proline-rich domain (Fig. 9K), was also detected in the nuclei.

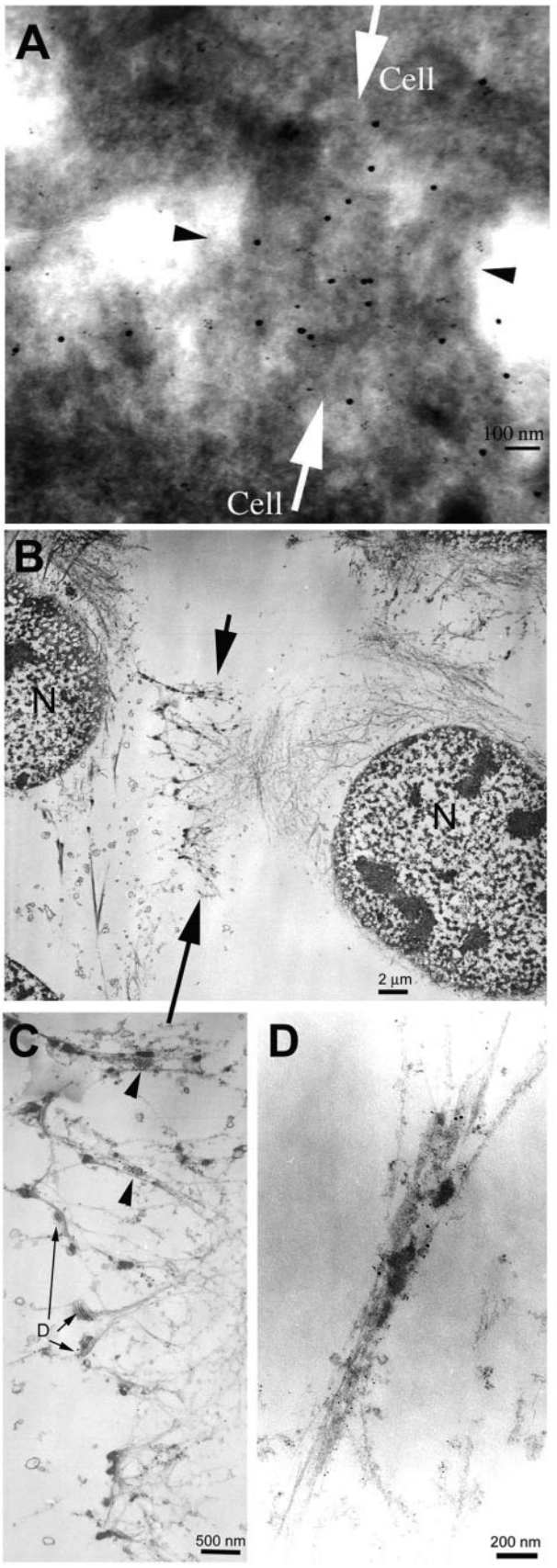

Mig-2 localizes to cell-ECM but not cell-cell adhesions

The finding that the C-terminal LIM domains, to which Mig-2 binds, mediate migfilin localization to cell-cell junctions prompted us to test whether Mig-2 also localizes to cell-cell junctions. To do this, we stained primary human keratinocytes with a monoclonal anti-Mig-2 antibody. The results showed that Mig-2 is clustered at cell-ECM adhesions (Fig. 9A, arrowheads) where actin filaments were anchored (Fig. 9B). Mig-2, however, was not clustered at junctions between the neighboring cells (Fig. 9A, arrow), suggesting that Mig-2 is not responsible for recruiting migfilin to cell-cell junctions. Furthermore, these results suggest that the binding of Mig-2 to migfilin is insufficient for recruiting Mig-2 to cell-cell junctions.

The LIM 2 and LIM3 domains, but not the LIM1 domain, are required for migfilin clustering at cell-ECM adhesions

We previously showed that the migfilin C-terminal region

Fig. 4. Immunoelectron microscopic analyses of migfilin clusters at cell-cell junctions. Immunoelectron microscopic analysis of HaCat cells was performed as described in Materials and Methods. Cell adhesions connecting the two cells are shown in the orientation between the two open arrows. Note that the anti-β-catenin antibody (10 nm gold) and the anti-migfilin antibody (5 nm gold) were colocalized at areas of cell-cell contacts (between arrowheads). (B,C) Single pre-embedding immunotransmission microscopic images of HaCat cells at low (B) and high (C) magnification. In B, migfilin (beads) was clustered and associated with the actin bundles at cell-cell junctions (arrows). N indicates the nuclei of two neighboring cells. In C, desmosomes are indicated by arrows, and migfilin clusters are shown by arrowheads. Note that migfilin clusters were associated with the actin bundles but not desmosomes. (D) HaCat cells were prepared for pre-embedding immunotransmission microscopy and double stained with anti-migfilin and anti-β-catenin antibodies. Note that migfilin (10 nm gold particles) and β-catenin (5 nm gold particles) were closely clustered with the actin bundles.

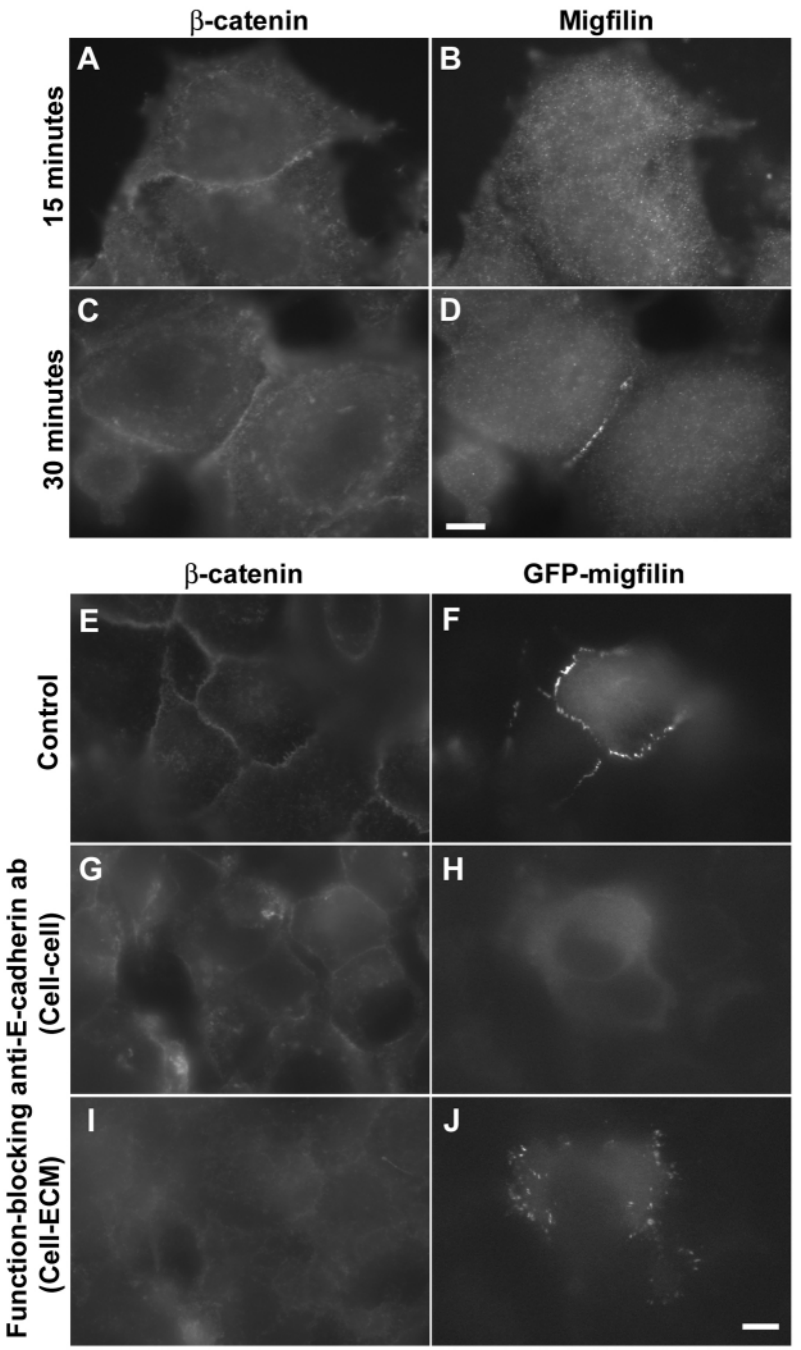

Fig. 5. Calcium-induced migfilin localization to adherens junction. (A-D) MCF7 mammary epithelial cells were subject to calcium-chelation assay as described in Materials and Methods. The cells were fixed at 15 minutes (A and B) and 30 minutes (C and D) after switching to calcium-containing medium, and double stained with a rabbit anti-β-catenin antibody (A and C) and the mouse monoclonal anti-migfilin antibody (B and D). (E,F) MCF7 mammary epithelial cells were transiently transfected with an expression vector encoding GFP-migfilin. The cells were subject to calcium-chelation assay in the presence of a function-blocking mouse monoclonal anti-E-cadherin antibody (SHE78-7) (G-J) or a non-specific mouse IgG as a control (E and F) as described in Materials and Methods. The cells were fixed at 60 minutes after switching to calcium-containing medium, and stained with a rabbit anti-β-catenin antibody (E, G and I) and a Rhodamine Red™-conjugated anti-rabbit IgG antibody. β-Catenin (E, G and I) and GFP-migfilin (F, H and J) at the cell-cell (E-H) or cell-ECM (I and J) adhesions were detected using a Leica DM R fluorescence microscope. Bars, 5 μm.

mediates its localization to cell-ECM adhesions (Tu et al., 2003). The specific LIM domains that are involved in the migfilin localization to cell-ECM adhesions, however, had not been determined. To identify the site that mediates migfilin localization to cell-ECM adhesions, we transfected HaCat cells with expression vectors encoding the wild-type or mutant forms of migfilin (Fig. 6) and stained the transfectants with the monoclonal anti-Mig-2 antibody. The results showed that, as expected, GFP-migfilin(s) (Fig. 9C) and GFP-migfilin (not shown) localize to cell-cell adhesions as well as cell-ECM adhesions. In addition, abundant GFP-migfilin(s) was detected in the nuclei (Fig. 9C). Consistent with the results obtained with primary keratinocytes (Fig. 9A), Mig-2 was co-clustered with migfilin in HaCat cells in cell-ECM adhesions but not cell-cell adhesions or the nuclei (Fig. 9D). GFP-ΔLIM1N, which lacks the first zinc finger of the LIM1 domain, was clustered at cell-cell adhesions (Fig. 9E, arrows) as well as cell-ECM adhesions (Fig. 9E, arrowheads), where Mig-2 was detected (Fig. 9F), suggesting that the first zinc finger of migfilin LIM1 domain is not required for the cell-ECM adhesion localization. The C243 (Fig. 9G), C291 (Fig. 9I), C306 (Fig. 9K) or C306(s) (not shown) mutants, however, were not clustered at cell-ECM adhesions where abundant Mig-2 was detected, although they were associated with the actin filaments. Thus, LIM2 and LIM3, but not LIM1, are required for migfilin clustering at cell-ECM adhesions.

Depletion of migfilin compromises the organization of adherens junctions

We next tested whether migfilin is required for the proper organization of adherens junctions. Human HT-1080 fibrosarcoma cells were selected for these studies because (1) previous studies have shown that these cells form extensive β-catenin-containing adherens junctions (Chitaev and Troyanovsky, 1997; Sacco et al., 1995), (2) our preliminary studies have shown that migfilin is recruited to the β-catenin-containing adherens junctions in these cells (see below) and (3) the level of migfilin in HT-1080 cells can be effectively reduced by RNA interference (see below). To suppress the expression of migfilin, we transfected HT-1080 cells with an siRNA that specifically targets migfilin mRNA (Tu et al., 2003). Western blot analyses showed that the migfilin siRNA reduced the cellular level of migfilin by more than 50% (Fig. 10A, lanes 1 and 2). Equal loading was confirmed by probing the same samples with an anti-actin antibody (Fig. 10B, lanes 1 and 2). Consistent with previous studies (Chitaev and Troyanovsky, 1997; Sacco et al., 1995), abundant β-catenin was detected in HT-1080 cells (Fig. 10C, lane 1). The level of β-catenin, unlike that of migfilin, was not reduced in the presence of the migfilin siRNA (Fig. 10C, lane 2),

further confirming the equal loading and the specificity of the migfilin siRNA.

Consistent with previous studies (Chitaev and Troyanovsky, 1997; Sacco et al., 1995), extensive β-catenin-containing adherens junctions were formed in HT-1080 cells that express a normal level of migfilin (Fig. 10D,F). Immunofluorescent staining of HT-1080 cells with a rabbit polyclonal anti-β-catenin antibody and a mouse monoclonal anti-migfilin antibody showed that, as expected, a substantial amount of migfilin was co-clustered with β-catenin at cell-cell junctions (Fig. 10, compare F and H). Noticeably, suppression of migfilin expression by RNA interference substantially impaired the organization of the β-catenin-containing adherens junctions (Fig. 10E,G,I), albeit the total cellular level of β-catenin was not reduced in these cells (Fig. 10C). Thus, migfilin is involved in the regulation of the organization of the β-catenin-containing adherens junctions but not the expression of β-catenin. Interestingly, migfilin-containing cell-ECM adhesions, unlike adherens junctions, were not eliminated in the migfilin siRNA transfectants under the experimental condition used, although they appeared somewhat smaller than those in the control cells (Fig. 10J,K). We next analyzed the effects of depletion of migfilin on F-actin and cadherin, another marker of cell-cell adhesions. To do this, we dually stained the cells with phalloidin and the monoclonal anti-migfilin antibody, or a rabbit polyclonal anti-β-catenin antibody and a mouse monoclonal anti-cadherin antibody. In control cells that express a normal level of migfilin, abundant F-actin was detected at cell-cell junctions where a substantial fraction was associated with clusters of migfilin (Fig. 11D,F,H). Furthermore, as expected, β-catenin and cadherin are co-clustered at cell-cell junctions (Fig. 11J,L,N). By contrast, in migfilin siRNA transfectants that express a reduced level of migfilin, the actin cytoskeleton was disorganized (Fig. 11, compare H and I) and β-catenin and cadherin distributed rather diffusely in the cells (Fig. 11K,M,O). In parallel experiments, western blotting analyses showed that the cellular cadherin level (Fig. 11C, lanes 1 and 2), like that of β-catenin (Fig. 10C, lanes 1 and 2), was not significantly reduced in migfilin siRNA transfectants in which the expression of migfilin was

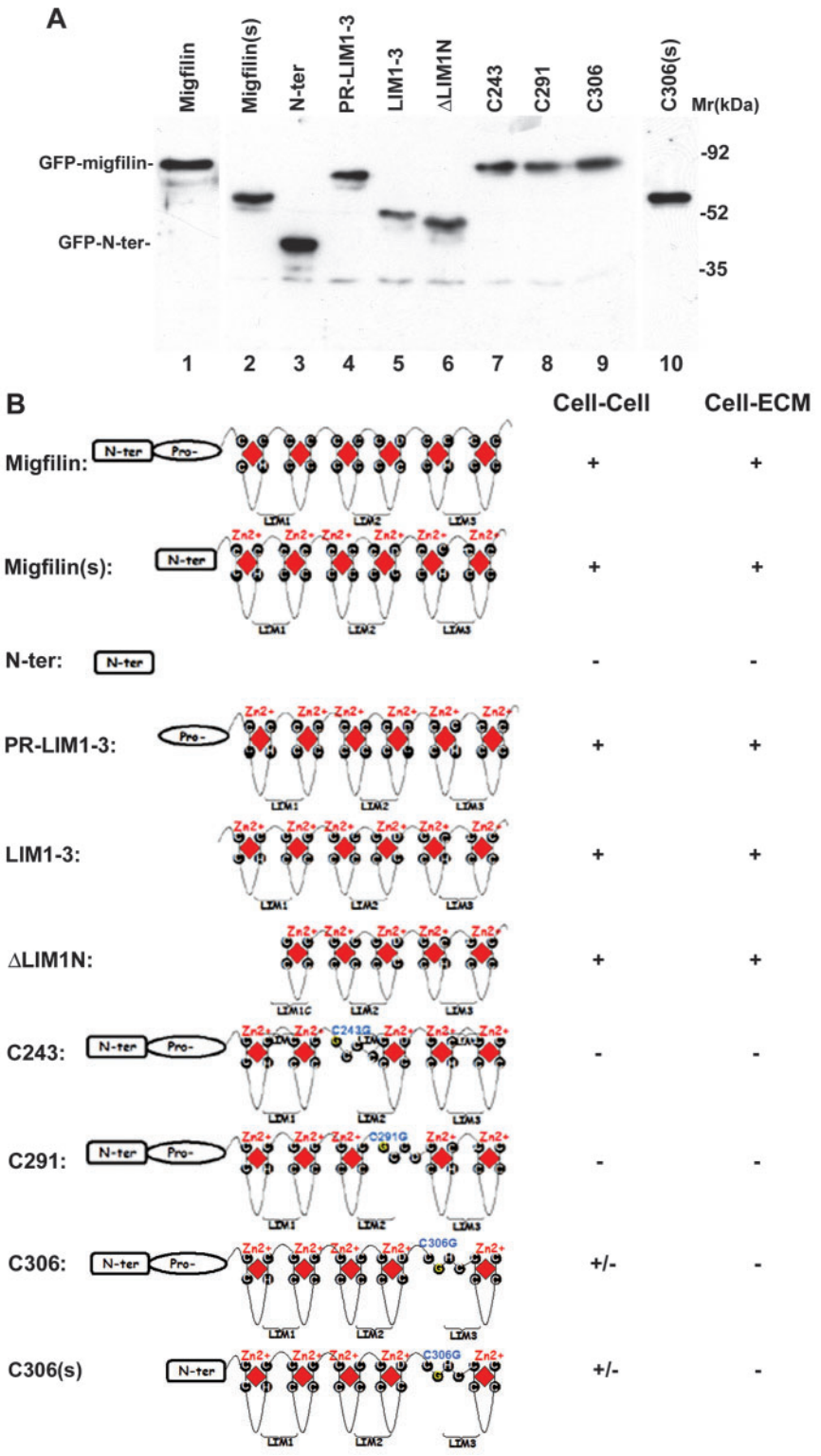

Fig. 6. Expression and schematic representation of the wild-type and mutant forms of migfilin and their localization to cell-cell and cell-ECM adhesions. (A) Expression of GFP-tagged wild-type and mutant forms of migfilin. HyCat cells were transfected with expression vectors encoding the wild-type and mutant forms of migfilin as indicated in the figure. The cell lysates (15 μg/lane) were analyzed by western blotting with an anti-GFP antibody. N-ter, residues 1-85; PR-LIM1-3, residues 85-373; LIM1-3, residues 176-373; ΔLIM1N, residues 205-373; C243, C291 and C306, migfilin bearing C243→G, C291→G or C306→G point mutation. C306(s), migfilin(s) bearing the C306→G point mutation. (B) Summary of the localization of the wild-type and mutant forms of migfilin to cell-cell and cell-ECM adhesions, based on the results presented in this paper.

suppressed (Fig. 11A, lanes 1 and 2). Taken together, these results suggest that migfilin is crucially involved in the proper organization of adherens junctions.

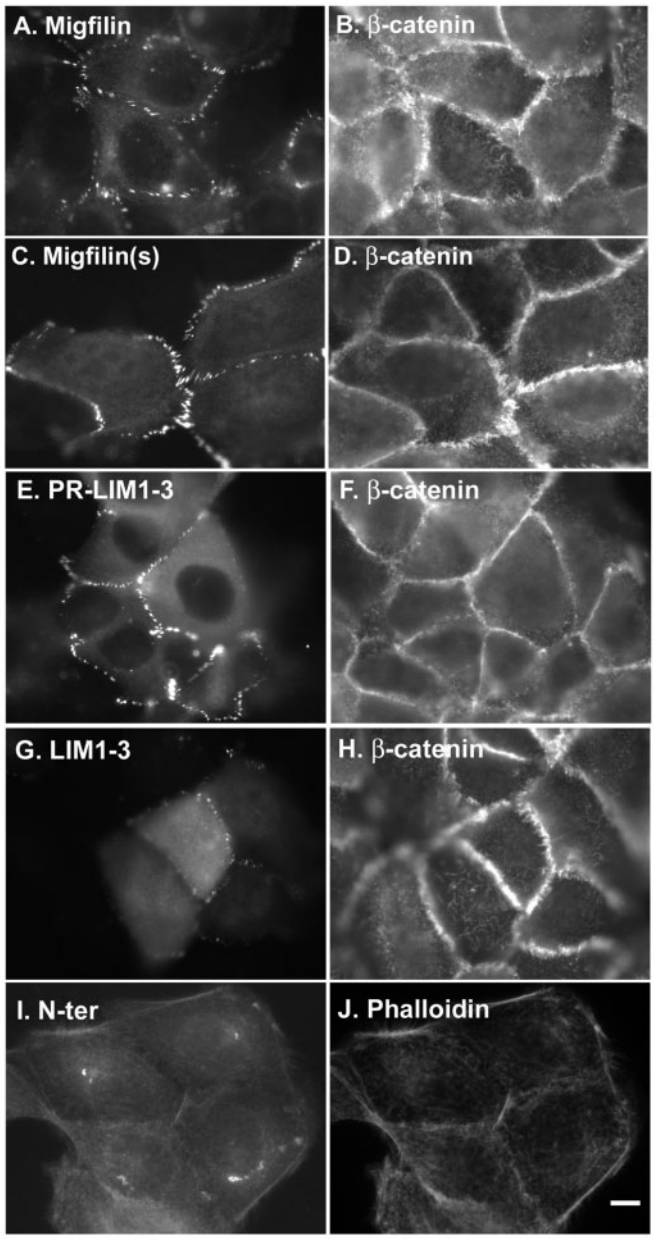

Fig. 7. The C-terminal LIM domains, but not the N-terminal filamin-binding domain or the central proline-rich domain, mediate migfilin localization to adherens junctions. (A-D) The central proline-rich domain is not required for migfilin localization to cell-cell junctions. HaCat cells were transfected with expression vectors encoding GFP-migfilin (A and B) or GFP-migfilin(s) (C and D). The cells were stained with the rabbit anti-β-catenin primary antibody and Rhodamine Red™-conjugated anti-rabbit IgG secondary antibody, and were observed under a Leica DM R fluorescence microscope equipped with GFP (A and C) or rhodamine (B and D) filters. (E-J) The C-terminal LIM domains, but not the N-terminal filamin-binding domain, are sufficient for mediating migfilin localization to adherens junctions. HaCat cells that were transiently transfected with expression vectors encoding GFP-PR-LIM1-3 (E and F), GFP-LIM1-3 (G and H) or GFP-N-ter (I and J) were stained with the anti-β-catenin antibody or phalloidin as indicated. Bar, 8 μm.

To further assess the function of migfilin in cell-cell adhesion, we analyzed the parental HT-1080 cells, the control RNA transfectants and the migfilin siRNA transfectants using a cell dissociation assay. To do this, the cells were detached from culture plates with a rubber policeman and passed through Pasteur pipettes ten times. The majority of the migfilin siRNA transfectants, which expressed a reduced level of migfilin (Fig. 12A, lane 3), were dissociated from each other after pipetting (Fig. 12,C,F). By contrast, under identical experimental conditions, significantly higher percentages of the control cells (i.e. the parental HT-1080 cells and the control RNA transfectants) that express a normal level of migfilin (Fig.

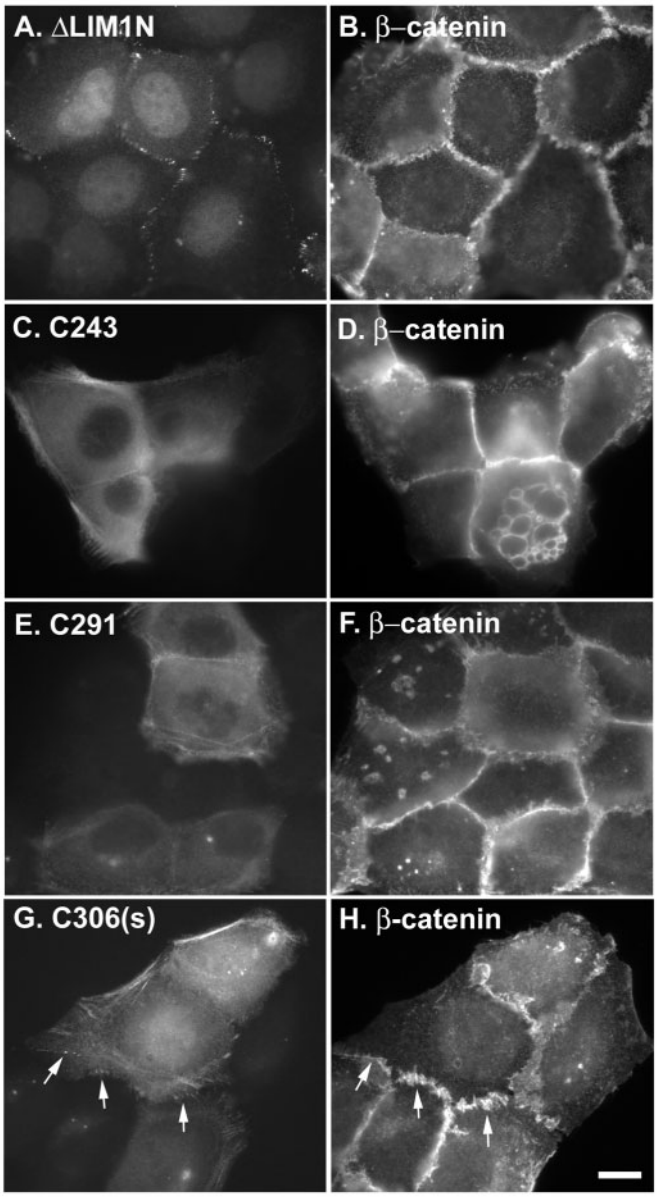

Fig. 8. LIM2 is essential for migfilin localization to adherens junctions. HaCat cells were transfected with the expression vectors encoding GFP-ΔLIM1N (A), GFP-C243 (C), GFP-C291 (E) and GFP-C306(s) (G). The cells were stained with the anti-β-catenin antibody as indicated (B, D, F and H). Notice that a small amount of GFP-tagged C306(s) mutant was detected in b-catenin-rich adherens junctions (G and H, arrows). Bar, 8 μm.

12A, lanes 1 and 2) remained associated with each other (Fig. 12D,E,F). Thus, consistent with the disorganization of β-catenin and cadherin (Fig. 11), depletion of migfilin weakened the cell-cell association.

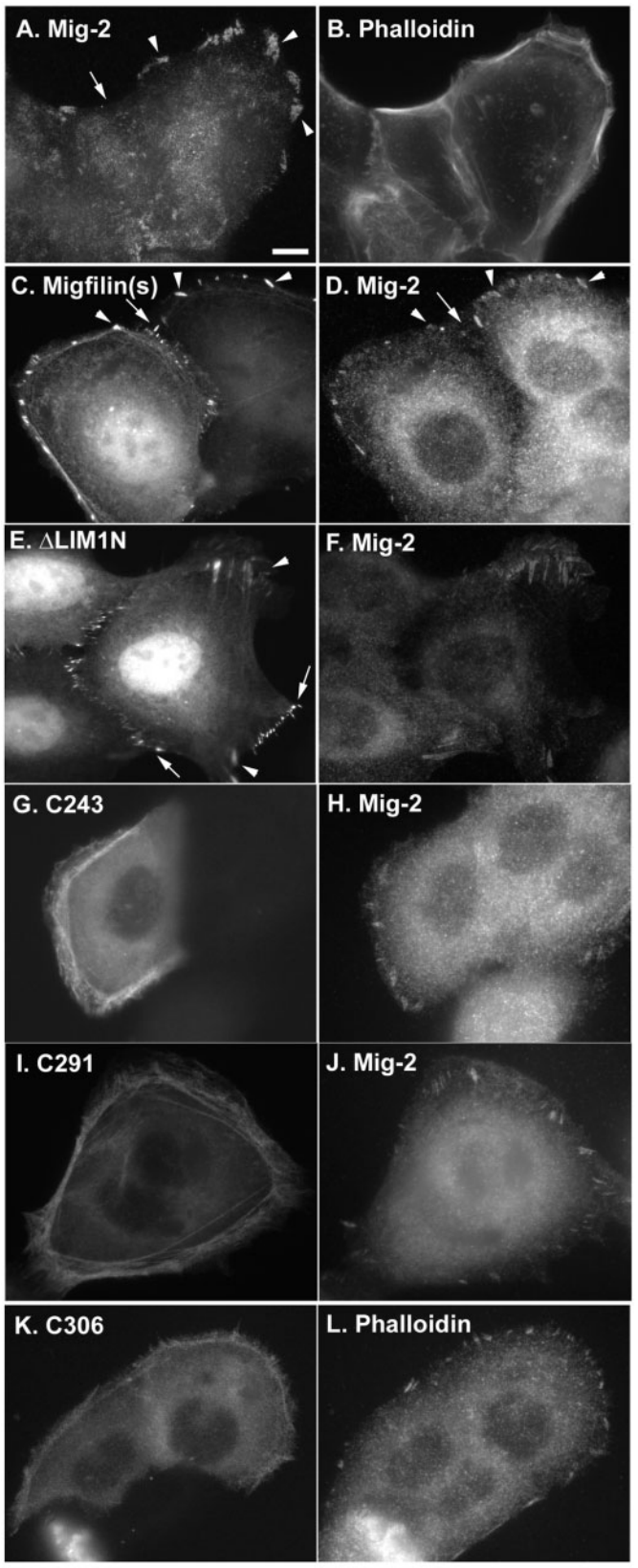

Discussion

Cell-cell junctions are highly specialized subcellular structures that are essential for epithelial and endothelial tissue formation and communication between neighboring cells. The studies presented in this paper have identified a new component of cell-cell junctions. Migfilin was identified and cloned based on its interaction with Mig-2, an important component of cell-ECM adhesions (Tu et al., 2003). In adherent cells lacking cell-cell junctions, migfilin is largely co-localized with Mig-2 at cell-ECM adhesions (Tu et al., 2003). Using a combination of biochemical, cell biological, immunofluorescence and immunoelectron microscopic approaches, we have now shown that in epithelial as well as endothelial cells, migfilin localizes not only to cell-ECM adhesions but also to cell-cell junctions.

In addition to showing that migfilin is a component of cell-cell junctions, we have characterized, both temporally and spatially, the localization of migfilin to cell-cell junctions. Migfilin localizes to cell-cell junctions soon after calcium-induced clustering of cadherin-β-catenin complex at these sites, suggesting that the localization of migfilin to cell-cell junctions is probably triggered by the presence of cadherin-β-catenin complex at these sites. Importantly, immunoelectron microscopic analyses have shown that migfilin is co-clustered with β-catenin at cell-cell junctions. These findings raise an interesting possibility that migfilin binds to β-catenin or other components of the cadherin-β-catenin complex at adherens junctions, resulting in the formation of a supramolecular complex containing migfilin, β-catenin and other components of adherens junctions.

Using an siRNA-mediated knockdown approach, we have found that migfilin is functionally indispensable for proper organization of adherens junctions. It is worth noting that whereas the migfilin- and β-catenin-containing adherens junctions were largely eliminated in HT-1080 cells in which the expression of migfilin is suppressed, a substantial number of migfilin-containing cell-ECM adhesions were detected in the cells that lacked migfilin- and β-catenin-containing adherens junctions. These results suggest that the dynamics of these two migfilin-containing adhesion structures (i.e. cell-cell and cell-ECM adhesions) are probably different. Migfilin in the cell-cell adhesions probably has a faster turnover rate than that in cell-ECM adhesions and therefore inhibition of migfilin synthesis by RNA interference resulted in a more dramatic down-regulation of migfilin at cell-cell adhesions and consequently the loss of adherens junctions. The loss of adherens junctions induced by the preferential elimination of migfilin at cell-cell adhesions in response to siRNA-mediated suppression of migfilin expression strongly suggests a direct

Fig. 9. Effects of point mutations within the LIM domains on migfilin localization to cell-ECM adhesions. (A-D) Mig-2 localizes to cell-ECM but not cell-cell adhesions. Primary newborn human embryonic keratinocytes were double stained with mouse monoclonal anti-Mig-2 antibody 3A3 (A) and phalloidin (B). HaCat cells that were transiently transfected with the GFP-migfilin(s) vector (C) were stained with the mouse monoclonal anti-Mig-2 antibody (D). (E-L) HaCat cells that were transiently transfected with expression vectors encoding GFP-tagged migfilin mutants (as indicated) were stained with the mouse monoclonal anti-Mig-2 antibody (F, H, J and L). Bar, 8 μm.

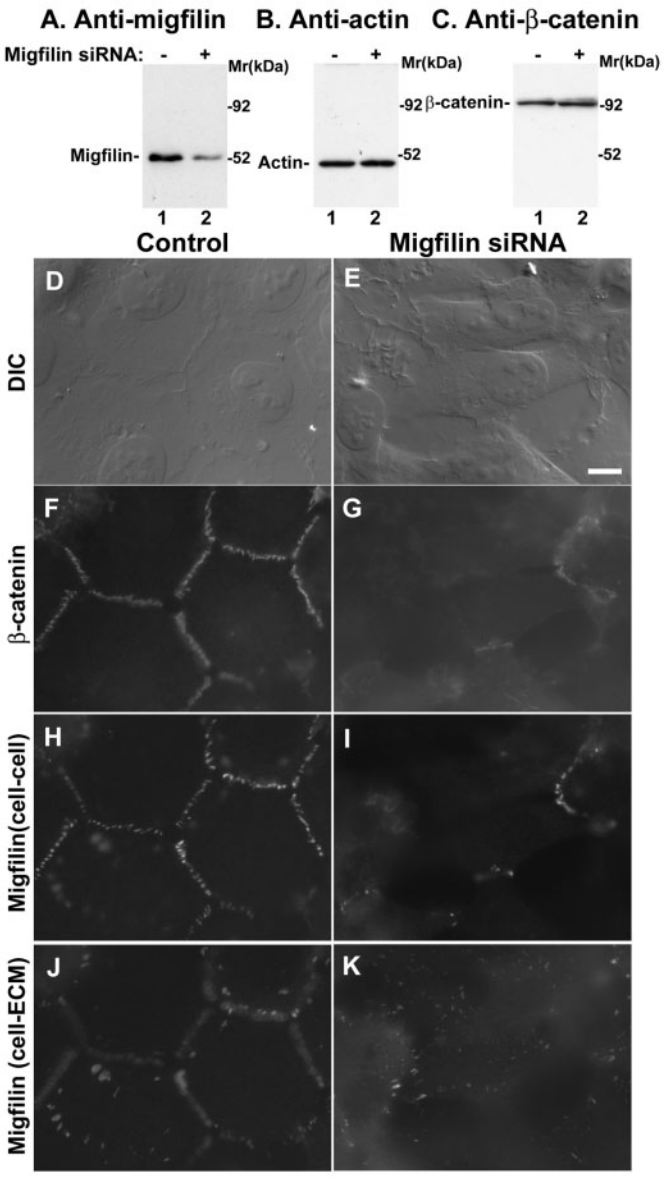

Fig. 10. siRNA-mediated depletion of migfilin and its effect on β-catenin organization. Human HT-1080 cells that were transfected with the migfilin siRNA (lane 2) or the control small RNA (lane 1) were analyzed by western blotting with monoclonal anti-migfilin antibody (clone 43) (A), monoclonal anti-actin antibody (B) or a polyclonal anti-β-catenin antibody (C). (D-K) HT-1080 cells transfected with the control RNA (D, F, H and J) or the migfilin siRNA (E, G, I and K) were double stained with mouse monoclonal anti-migfilin antibody (clone 43) (H-K) and rabbit-polyclonal anti-β-catenin antibody (F and G). The differential interference contrast (DIC) (D and E) and immunofluorescent (F-K) images were recorded using a Leica DM R fluorescence microscope equipped with a Hamamatsu ORCA-ER digital camera. Bar, 8 μm.

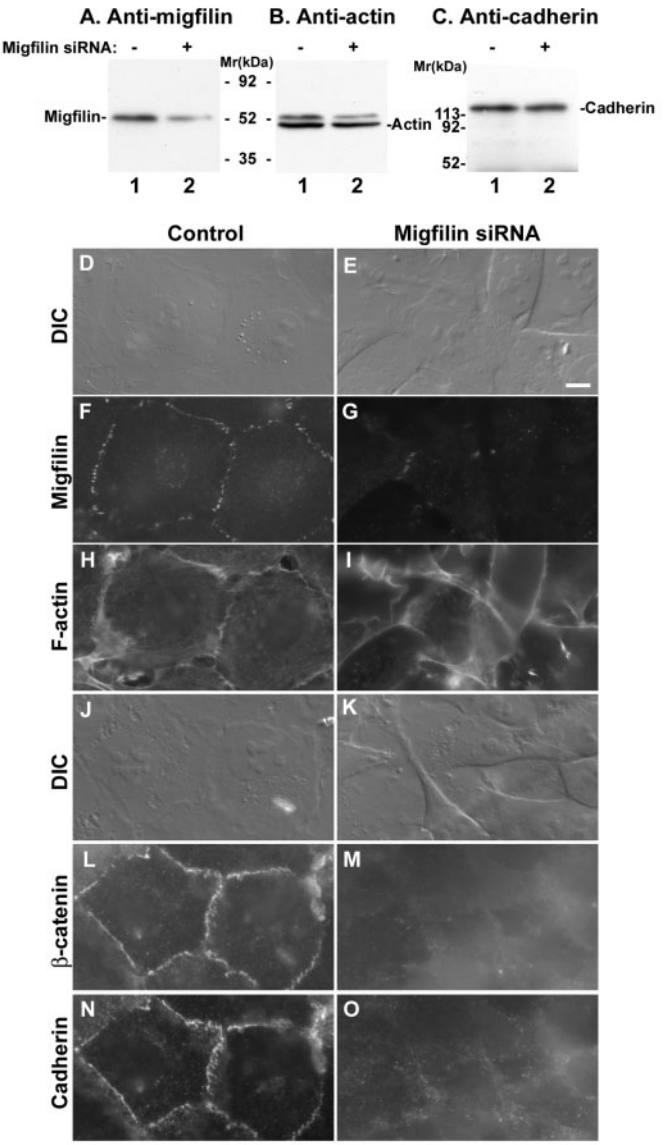

Fig. 11. Depletion of migfilin compromises the organization of adherens junctions. Human HT-1080 cells that were transfected with the migfilin siRNA (lane 2) or the control small RNA (lane 1) were analyzed by western blotting with monoclonal anti-migfilin antibody (clone 43) (A) or an anti-cadherin antibody (C). Equal loading was confirmed by re-probing the migfilin membrane (A) with a monoclonal anti-actin antibody (B). (D-I) HT-1080 cells transfected with the control RNA (D, F and H) or the migfilin siRNA (E, G and I) were double stained with the mouse monoclonal anti-migfilin antibody (clone 43) (F and G) and Rhodamine-conjugated phalloidin (H and I). The mouse anti-migfilin primary antibody was detected with a FITC-conjugated anti-mouse IgG secondary antibody. (J-O) HT-1080 cells transfected with the control RNA (J, L and N) or the migfilin siRNA (K, M and O) were double stained with a rabbit polyclonal anti-β-catenin antibody (L and M) and a mouse monoclonal anti-cadherin antibody (clone CH-19) (N and O). The DIC (D, E, J and K) and immunofluorescent (F-I and L-O) images were recorded as described in Fig. 10. Bar, 8 μm.

role of migfilin in the organization or maintenance of the cell-cell adhesion structure. Consistent with this, siRNA-mediated depletion of migfilin significantly weakened the association of HT-1080 cells.

How does migfilin contribute to the organization or maintenance of adherens junctions? One characteristic of the migfilin-containing cell-cell adhesion structure is that it is highly resistant to detergent extraction, probably because of its cross-linking with filamentous actin at the adhesion sites

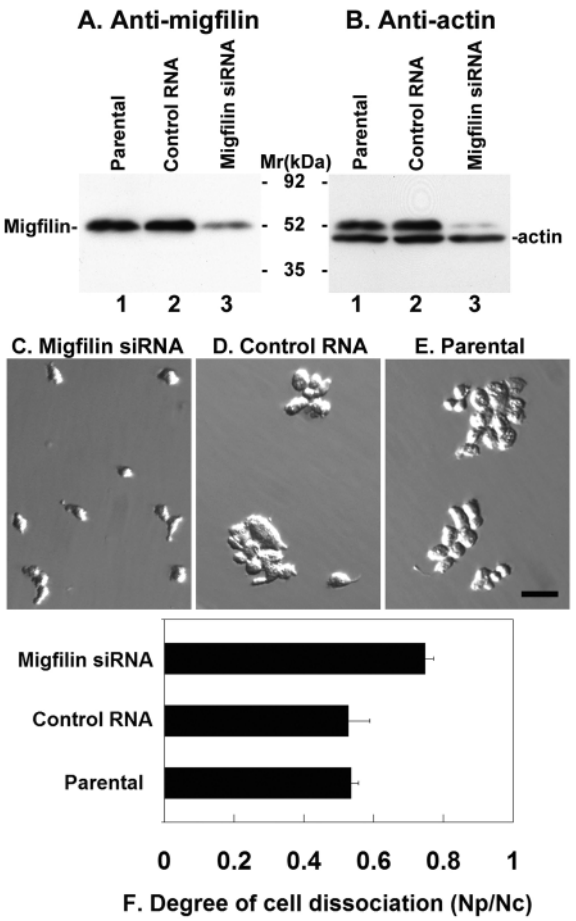

Fig. 12. Depletion of migfilin weakens the cell-cell association. (A,B) The parental HT-1080 cells (lane 1) and HT1080 cells that were transfected with the control small RNA (lane 2) or the migfilin siRNA (lane 3) were analyzed by western blotting with the monoclonal anti-migfilin antibody (A). Equal loading was confirmed by re-probing the membrane with an anti-actin antibody (B). (C-F) Cell dissociation. The migfilin siRNA transfectants (C), control RNA transfectants (D) and the parental HT-1080 cells (E) were detached from culture plates, passed through Pasteur pipettes ten times and observed under an Olympus IX70 inverted microscope. Bar in E, 100 μm. The degree of cell dissociation (the number of particles (Np)/the number of total cells (Nc)) was calculated by analyzing at least 500 cells from each sample (F). Bars in F represent means + s.d. from two independent experiments.

(Fig. 4). Migfilin interacts with two important actin-binding proteins, VASP (Y.Z., Y.T. and C.W., unpublished observation) and filamin (Tu et al., 2003; Takafuta et al., 2003). VASP, which binds to the central proline-rich domain of migfilin, is known to localize to adherens junctions (Grevengoed et al., 2002; Vasioukhin et al., 2000). However, VASP is unlikely to be responsible for recruiting migfilin to adherens junctions, as migfilin(s), which lacks the VASP-binding domain, also localizes to adherens junctions. Although VASP is unlikely to be functioning in mediating migfilin localization to adherens junction, it is possible that migfilin, through its interaction with VASP, functions in recruiting VASP to adherens junctions. Given the importance of VASP in the assembly and functions of epithelia (Comerford et al., 2002; Grevengoed et al., 2002; Lawrence et al., 2002; Vasioukhin et al., 2000), it will be interesting to test in future studies whether migfilin plays such a role. Migfilin, through its N-terminal domain, binds to filamin (Tu et al., 2003; Takafuta et al., 2003). The interaction of migfilin with filamin is probably responsible for the tight association of migfilin with actin filaments, as a migfilin fragment containing the filamin-binding N-terminal domain but lacking the central proline-rich domain and the C-terminal LIM domains stably associates with actin filaments in cells (Fig. 7I,J). Filamin cross-links actin filaments and is known to be crucial for the organization of the actin cytoskeleton (reviewed by Stossel et al., 2001; van der Flier and Sonnenberg, 2001). Additionally, filamin binds to Cdc42, Rac, Rho and guanine nucleotide exchange factors that regulate the small GTPases (Bellanger et al., 2000; Ohta et al., 1999) and their effectors such as p21-activated kinase (PAK) (Vadlamudi et al., 2002) and Rho-kinase (ROCK) (Ueda et al., 2003). There is strong evidence now for a crucial role of actin polymerization and their regulators such as Cdc42 and Rac in the assembly as well as the signaling of cell-cell adhesions (reviewed by Adams and Nelson, 1998; Braga, 2002; Jamora and Fuchs, 2002; Perez-Moreno et al., 2003). It is likely that the interaction of migfilin with filamin contributes to the organization, maintenance or signaling of the intercellular adhesions. Thus, the identification of migfilin as a functionally important component of adherens junctions and its characterization described in this paper shall facilitate future studies aimed at fully understanding the organization and signaling of this important adhesion structure.

In the present study, we have also identified the determinants that control migfilin localization to cell-cell and cell-ECM adhesions, two functionally coordinated but structurally distinct adhesion structures. Both LIM2 and LIM3 are crucially involved in the localization of migfilin to cell-cell and cell-ECM adhesions, whereas LIM1 (at least the first zinc finger of LIM1) is not required for migfilin localization to either adhesion site. These results suggest that the sites that control the distribution of migfilin to cell-cell and cell-ECM adhesions are largely overlapping. Importantly, Mig-2, which recruits migfilin to cell-ECM adhesions, is present exclusively in cell-ECM adhesions (Fig. 9). Thus, it is attractive to propose a model in which Mig-2 competes with the components of adherens junction for interacting with migfilin. In cells with both cell-cell and cell-ECM adhesions, there exist at least two pools of migfilin. One pool of migfilin binds to Mig-2, which results in the recruitment of migfilin to cell-ECM adhesions, whereas the second pool of migfilin associates with components of adherens junction and therefore is recruited to cell-cell adhesions. Thus, an elevation of the Mig-2 level could translate into upregulation of migfilin localization to cell-ECM adhesions and concomitantly downregulation of migfilin localization to cell-cell junctions. The coupling or 'cross-talking' between cell-cell and cell-ECM adhesions is crucial for several biological and pathological processes including epithelial-mesenchymal transition, wound healing, and carcinoma invasion. The 'competition' model of migfilin localization to cell-cell and cell-ECM adhesions could provide a potential mechanism by which cells coordinately regulate the assembly or signaling of cell-cell and cell-ECM adhesions.

We thank Dr Fengli Guo for technical assistance in the immunoelectron microscopic analyses. This work was supported by NIH grants GM65188 and DK54639 to C.W. and CA76541 to D.B.S.

References

Adams, C. L. and Nelson, W. J. (1998). Cytomechanics of cadherin-mediated cell–cell adhesion. *Curr. Opin. Cell Biol.* **10**, 572-577.

Akazawa, H., Kudoh, S., Mochizuki, N., Takekoshi, N., Takano, H., Nagai, T. and Komuro, I. (2004). A novel LIM protein Cal promotes cardiac differentiation by association with CSX/NKX2-5. *J. Cell Biol.* **164**, 395-405.

Bellanger, J. M., Astier, C., Sardet, C., Ohta, Y., Stossel, T. P. and Debant, A. (2000). The Rac1- and RhoG-specific GEF domain of Trio targets filamin to remodel cytoskeletal actin. *Nat. Cell Biol.* **2**, 888-892.

Braga, V. M. M. (2002). Cell-cell adhesion and signalling. *Curr. Opin. Cell Biol.* **14**, 546-556.

Burridge, K. and Chrzanowska-Wodnicka, M. (1996). Focal adhesions, contractility, and signaling. *Annu. Rev. Cell Dev. Biol.* **12**, 463-518.

Chaney, L. K. and Jacobson, B. S. (1983). Coating cells with colloidal silica for high yield isolation of plasma membrane sheets and identification of transmembrane proteins. *J. Biol. Chem.* **258**, 10062-10072.

Chen, Y. T., Stewart, D. B. and Nelson, W. J. (1999). Coupling assembly of the E-cadherin/beta-catenin complex to efficient endoplasmic reticulum exit and basal-lateral membrane targeting of E-cadherin in polarized MDCK cells. *J. Cell Biol.* **144**, 687-699.

Chitaev, N. A. and Troyanovsky, S. M. (1997). Direct Ca^{2+}-dependent heterophilic interaction between desmosomal cadherins, desmoglein and desmocollin, contributes to cell-cell adhesion. *J. Cell Biol.* **138**, 193-201.

Comerford, K. M., Lawrence, D. W., Synnestvedt, K., Levi, B. P. and Colgan, S. P. (2002). Role of vasodilator-stimulated phosphoprotein in PKA-induced changes in endothelial junctional permeability. *FASEB J.* **16**, 583-585.

Dawid, I. B., Breen, J. J. and Toyama, R. (1998). LIM domains: multiple roles as adapters and functional modifiers in protein interactions. *Trends Genet.* **14**, 156-162.

Geiger, B., Bershadsky, A., Pankov, R. and Yamada, K. M. (2001). Transmembrane crosstalk between the extracellular matrix–cytoskeleton crosstalk. *Nat. Rev. Mol. Cell Biol.* **2**, 793-805.

Grevengoed, E. E., Price, M. H., McCartney, B. M., Hayden, M. A., DeNofrio, J. C. and Peifer, M. (2002). Abelson kinase regulates epithelial morphogenesis in Drosophila. *Dev. Biol.* **250**, 91-100.

Helwani, F. M., Kovacs, E. M., Paterson, A. D., Verma, S., Ali, R. G., Fanning, A. S., Weed, S. A. and Yap, A. S. (2004). Cortactin is necessary for E-cadherin-mediated contact formation and actin reorganization. *J. Cell Biol.* **164**, 899-910.

Heuser, J. E. and Kirschner, M. W. (1980). Filament organization revealed in platinum replicas of freeze-dried cytoskeletons. *J. Cell Biol.* **86**, 212-234.

Hynes, R. O. (2002). Integrins: bidirectional, allosteric signaling machines. *Cell* **110**, 673-687.

Jamora, C. and Fuchs, E. (2002). Intercellular adhesion, signalling and the cytoskeleton. *Nat. Cell Biol.* **4**, E101-E108.

Jurata, L. W. and Gill, G. N. (1998). Structure and function of LIM domains. *Curr. Top. Microbiol. Immunol.* **228**, 75-113.

Krause, M., Dent, E. W., Bear, J. E., Loureiro, J. J. and Gertler, F. B. (2003). Ena/VASP proteins: regulators of the actin cytoskeleton and cell migration. *Annu. Rev. Cell Dev. Biol.* **19**, 541-564.

Lawrence, D. W., Comerford, K. M. and Colgan, S. P. (2002). Role of VASP in reestablishment of epithelial tight junction assembly after Ca2+ switch. *Am. J. Phys. Cell Phys.* **282**, C1235-C1245.

Liu, S., Calderwood, D. A. and Ginsberg, M. H. (2000). Integrin cytoplasmic domain-binding proteins. *J. Cell. Sci.* **113**, 3563-3571.

Nagafuchi, A., Shirayoshi, Y., Okazaki, K., Yasuda, K. and Takeichi, M. (1987). Transformation of cell adhesion properties by exogenously introduced E-cadherin cDNA. *Nature* **329**, 341-343.

Ohta, Y., Suzuki, N., Nakamura, S., Hartwig, J. H. and Stossel, T. P. (1999). The small GTPase RalA targets filamin to induce filopodia. *Proc. Natl. Acad. Sci. USA* **96**, 2122-2128.

Perez-Moreno, M., Jamora, C. and Fuchs, E. (2003). Sticky business: orchestrating cellular signals at adherens junctions. *Cell* **112**, 535-548.

Rogalski, T. M., Mullen, G. P., Gilbert, M. M., Williams, B. D. and Moerman, D. G. (2000). The UNC-112 gene in Caenorhabditis elegans encodes a novel component of cell-matrix adhesion structures required for integrin localization in the muscle cell membrane. *J. Cell Biol.* **150**, 253-264.

Rothen-Rutishauser, B., Riesen, F. K., Braun, A., Gunthert, M. and Wunderli-Allenspach, H. (2002). Dynamics of tight and adherens junctions under EGTA treatment. *J. Membr. Biol.* **188**, 151-162.

Sacco, P. A., McGranahan, T. M., Wheelock, M. J. and Johnson, K. R. (1995). Identification of Plakoglobin domains required for association with N-cadherin and alpha-catenin. *J. Biol. Chem.* **270**, 20201-20206.

Schmeichel, K. L. and Beckerle, M. C. (1994). The LIM domain is a modular protein-binding interface. *Cell* **79**, 211-219.

Stolz, D. B. and Jacobson, B. S. (1992). Examination of transcellular membrane protein polarity of bovine aortic endothelial cells in vitro using the cationic colloidal silica microbead membrane-isolation procedure. *J. Cell. Sci.* **103**, 39-51.

Stossel, T. P., Condeelis, J., Cooley, L., Hartwig, J. H., Noegel, A., Schleicher, M. and Shapiro, S. S. (2001). Filamins as integrators of cell mechanics and signalling. *Nat. Rev. Mol. Cell Biol.* **2**, 138-145.

Takafuta, T., Saeki, M., Fujimoto, T. T., Fujimura, K. and Shapiro, S. S. (2003). A new member of the LIM protein family binds to filamin B and localizes at stress fibers. *J. Biol. Chem.* **278**, 12175-12181.

Takeda, H., Nagafuchi, A., Yonemura, S., Tsukita, S., Behrens, J., Birchmeier, W. and Tsukita, S. (1995). V-src kinase shifts the cadherin-based cell adhesion from the strong to the weak state and β-catenin is not required for the shift. *J. Cell Biol.* **131**, 1839-1847.

Tokuyasu, K. T. (1989). Use of poly(vinylpyrrolidone) and poly(viny lalcohol) for cryoultramicrotomy. *Histochem. J.* **21**, 163-171.

Tu, Y., Wu, S., Shi, X., Chen, K. and Wu, C. (2003). Migfilin and mig-2 link focal adhesions to filamin and the actin cytoskeleton and function in cell shape modulation. *Cell* **113**, 37-47.

Ueda, K., Ohta, Y. and Hosoya, H. (2003). The carboxy-terminal pleckstrin homology domain of ROCK interacts with filamin-A. *Biochem. Biophys. Res. Com.* **301**, 886-890.

Vadlamudi, R. K., Li, F., Adam, L., Nguyen, D., Ohta, Y., Stossel, T. P. and Kumar, R. (2002). Filamin is essential in actin cytoskeletal assembly mediated by p21-activated kinase 1. *Nat. Cell Biol.* **4**, 681-690.

van der Flier, A. and Sonnenberg, A. (2001). Structural and functional aspects of filamins. *Biochim. Biophys. Acta* **1538**, 99-117.

Vasioukhin, V., Bauer, C., Yin, M. and Fuchs, E. (2000). Directed actin polymerization is the driving force for epithelial cell-cell adhesion. *Curr. Opin. Cell Biol.* **100**, 209-219.

Yap, A. S., Brieher, W. M. and Gumbiner, B. M. (1997). Molecular and functional analysis of cadherin-based adherens junctions. *Annu. Rev. Cell Dev. Biol.* **13**, 119-146.

Zhang, Y., Chen, K., Tu, Y., Velyvis, A., Yang, Y., Qin, J. and Wu, C. (2002). Assembly of the PINCH-ILK-CH-ILKBP complex precedes and is essential for localization of each component to cell-matrix adhesion sites. *J. Cell Sci.* **115**, 4777-4786.